Effect of the Reynolds and Richardson Numbers on the Growth of Well-Aligned Ultralong Single-Walled Carbon Nanotubes

Banghua Peng,[†,‡] Yagang Yao,[†] and Jin Zhang*[,†]

Center for Nanochemistry, Beijing National Laboratory for Molecular Sciences (BNLMS), Key Laboratory for the Physics and Chemistry of Nanodevices, State Key Laboratory for Structural Chemistry of Unstable and Stable Species, College of Chemistry and Molecular Engineering, Peking University, Beijing 100871, People's Republic of China, and College of Chemistry and Chemical Engineering, Shihezi University, Xinjiang 832000, People's Republic of China

Received: April 26, 2010; Revised Manuscript Received: May 20, 2010

In this study, the effect of the Reynolds number (R_e) and Richardson number (R_i) on the growth of well-aligned ultralong single-walled carbon nanotubes (SWNTs) has been systematically investigated. Smaller R_e and larger R_i are favored for the growth of ultralong SWNTs by analyzing the fluid dynamical properties of chemical vapor deposition and the floating growth mode of ultralong SWNTs. Comparative experiments at different R_e and R_i were carried out by altering the inner diameter of the quartz tube and gas flux in different growth processes. Growth results indicated that either reducing the gas flux or increasing the inner diameter of the tube, which corresponds to smaller R_e or larger R_i, is beneficial for the growth of well-aligned ultralong SWNTs. On the other hand, too large a R_i, namely, a large buoyancy, is not suitable to grow parallel SWNT arrays for its disturbance to the laminar flow. The laminar flow and appropriate buoyancy are two vital factors for the growth of parallel and high-quality SWNT arrays.

Introduction

Single-walled carbon nanotubes (SWNTs) have been regarded as one of the best candidates for nanoelectronic devices due to their unique electronic structure and superior electrical properties.[1,2] Numerous nanoelectronic devices based on individual SWNT have been fabricated, such as field effect transistors,[3–5] logic gates,[6] inverters,[7] etc. However, a lot of challenges still remain in the structure-controlled growth of SWNTs,[8,9] as well as their device fabrication and integration.[10,11] To realize the fabrication of SWNT-based devices in a controlled manner, the crucial step is the direct synthesis of SWNTs on a surface with a controlled position and orientation.[12,13]

Generally, there are two widely utilized growth modes for horizontally aligned SWNTs: lattice-orientated growth mode[14,15] and gas flow-directed growth mode (kite-mechanism).[16] For the former one, high-density SWNT arrays can be obtained, although a special crystal substrate, such as quartz or sapphire, is required in this approach and the as-grown SWNTs have to be transferred onto other substrates for further device fabrication.[10,17–19] In contrast with lattice-orientated growth, centimeter-scale ultralong SWNTs can be achieved either on a silicon substrate or on others based on the latter growth mode. The as-grown well-aligned ultralong SWNTs on SiO_2/Si are preferred for fabrication of various nanodevices. Furthermore, electronic structure modulation can be realized in various areas along the same SWNT during the gas flow-directed growth mode,[20,21] which would be a significant advancement toward device integration.[22,23] By combining the two growth modes, a SWNT cross-bar, a promising structure for nonvolatile random access memory for molecular computing,[6] could be obtained in a one batch reaction.[24] Recently, some studies have been made to study the impact of gas flow direction on the SWNTs' growth,[25,26] especially for ultralong SWNTs.[27,28] However, many problems still exist in the accurate control of the orientation of ultralong SWNTs during the gas flow-directed growth process.

The gas flow-directed growth mode is regarded as a simple and fast approach to obtain well-aligned ultralong SWNTs arrays. Normally, two factors should be taken into consideration: gas flow in the quartz tube should be laminar, and growing SWNTs should enter the laminar flow. For the latter one, a "fast-heating" methane chemical vapor deposition (CVD)[16] approach was reported to create and enhance the temperature difference between the substrate and surrounding atmosphere. The buoyancy produced by the temperature difference can lift the catalysts or SWNTs up into the laminar flow and lead to the growth of millimeter-scale SWNTs. Four centimeter ultralong SWNTs were also achieved by ethanol-CVD[29] without the "fast-heating" step, indicating that the buoyancy is also large enough to lift catalysts or SWNTs up into the laminar flow in a "normal heating" CVD system.

In the present study, based on analysis of the fluid dynamical properties of the CVD system and the floating growth model of ultralong SWNTs, we found that the two factors, laminar gas flow and the lifting movement of SWNTs caused by buoyancy, should be taken into consideration simultaneously during the SWNTs' growth. Moreover, too large of a buoyancy is not suitable for orderly SWNT arrays for its disturbance to the laminar flow. Laminar gas flow and appropriate buoyancy are vital factors in the growth of ordered SWNTs with high quality. Experiments of the ultralong SWNTs' growth have been carried out at different Reynolds numbers (R_e) and Richardson numbers (R_i) by changing the inner diameter of the quartz tubes or the gas flux in the growth process. Growth results indicated that a smaller R_e (more stable gas flow) or a larger R_i (larger

* To whom correspondence should be addressed. Tel/Fax: 86-10-6275-7157. E-mail: jinzhang@pku.edu.cn.
[†] Peking University.
[‡] Shihezi University.

10.1021/jp103731p
Published on Web 07/08/2010

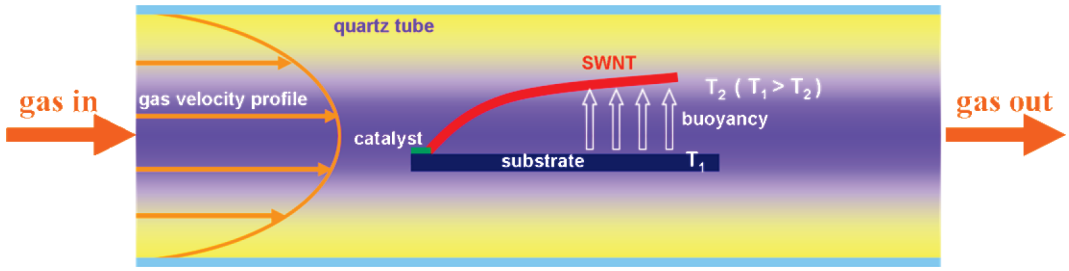

Figure 1. Schematic illustration of the CVD system for SWNT growth. The buoyancy, introduced by the temperature gradient, makes the SWNT float up from the substrate.

buoyancy), introduced by either reducing the gas flow flux or increasing the tube's inner diameter, is beneficial for the growth of SWNTs with high quality.

Experimental Details

A. Growth of Ultralong SWNTs. Ultralong SWNTs were grown in the ambient pressure CVD system (Lindberg Blue M tube furnace). $FeCl_3$ (0.01 M) (sometimes 0.01 M $CuCl_2$ or 0.01 M $MnCl_2$) in ethanol was used as a catalyst precursor, which was stamped by PDMS (polydimethyl siloxane) in strips on an 800 nm SiO_2/Si substrate. The substrates were put into the CVD system by arranging the substrate catalyst-side upward and catalyst lines facing the gas flow. The furnace was heated to 970 °C in 30 min under a flow of 30 sccm (sccm = standard cubic centimeters per minute) Ar and 80 sccm H_2. The catalyst precursor was then pretreated at 970 °C for 15 min, after which SWNTs were grown under different CH_4 and H_2 flows for another 30 min. Finally, the carbon feed was shut down and the sample was cooled to room temperature under the same flux of Ar as the total flux of CH_4 and H_2 in the growth process. Experiments were carried out in five different inner diameter quartz tubes, which were 12, 14, 18, 22, and 37 mm.

B. Characterization. Scanning electron microscopy (SEM) observations were carried out using a Hitachi S-4800 field emission scanning electron microscope. Micro-Raman spectroscopy (Renishaw 1000, assembled with a confocal imaging microscope with an excitation energy of 1.96 eV (632.8 nm)) was used to characterize the SWNTs, and the diameters of the SWNTs were estimated through atomic force microscopy (AFM) (NanoScope III, Veeco Co., U.S.A., operated at tapping-mode).

Results and Discussion

A. Analysis of the Growth Process of Well-Aligned Ultralong SWNTs. Figure 1 shows the schematic illustration of the sectional view of the CVD system for SWNT growth, where two issues should be considered for growing well-aligned ultralong SWNTs: how to get the stable laminar flow in the quartz tube and how to lift the catalysts or SWNTs up into the laminar flow. For the first one, the accepted well-judged parameter for laminar flow is the Reynolds number R_e[30]

$$R_e = \frac{\rho v d}{\mu} \tag{1}$$

where ρ represents the gas density, v represents the gas velocity, d represents the tube diameter, and μ represents the dynamic viscosity. To get a stable laminar gas flow, R_e must be less than 2000, according to fluid mechanics.[30] Furthermore, the smaller the R_e is, the more stable the gas flow will be. In the tube furnace system, the gas velocity v can be calculated by

$$v = \frac{4\phi}{\pi d^2} \tag{2}$$

Here, ϕ represents the gas flux and π is the Pi number. Displacing eq 2 into eq 1, R_e can be expressed by

$$R_e = \frac{4\rho\phi}{\pi\mu d} \tag{3}$$

Apparently, the R_e value is related to the gas flux ϕ and the tube diameter d. Deduced from eq 3, increasing the tube diameter or reducing the gas flux theoretically yields a smaller R_e value, which means that a more stable gas flow can be obtained.

However, in the actual process (see Figure 1), when the heated gas flow comes into the substrate, a velocity boundary layer and a heat boundary layer will be introduced, according to boundary theory in fluid mechanics.[30,31] It is also accepted that a large velocity and temperature variation existed within this boundary layer.[30] The temperature of the gas near the substrate surface (T_2) is lower than that of the substrate surface (T_1) due to a slow gas velocity, as well as a fast heat transfer of the gas near the substrate, which will bring about a temperature gradient. The temperature gradient will cause an extra motion between atmospheres with different gas densities. Usually, it is considered that buoyancy will be induced by the gas density variation, whereas a vertical convection action near the substrate arises along with buoyancy, which will disturb the stability of the laminar flow.[31]

In the CVD growth of SWNTs, buoyancy caused by a temperature gradient can overcome the binding effect of the substrate and spontaneously lift up the catalyst nanoparticles or the grown SWNTs into the laminar flow, thus leading to the synthesis of ultralong SWNTs.[32] Therefore, it is vital to keep a large buoyancy for SWNT growth. The buoyancy transportation can be scaled by the Richardson number R_i,[31] described by

$$R_i = \frac{\Delta\rho g h}{\rho v^2} \tag{4}$$

Here, $\Delta\rho$ represents the density difference in vertical length h with the gas velocity v and g represents the gravitational acceleration constant. R_i represents the buoyancy-to-inertia ratio in the heating fluid system. The larger the R_i is, the larger the buoyancy will be. Displacing v with the gas flux ϕ and the tube diameter d, R_i can be expressed by

$$R_i = \frac{\Delta\rho g h \pi^2 d^4}{16\rho\phi^2} \quad (5)$$

From the above expression, it can be observed that a large buoyancy can be obtained by increasing the tube diameter or decreasing the gas flux. To obtain well-aligned ultralong SWNTs, the buoyancy must be larger enough to assist the SWNTs floating up at first, and then the SWNTs will be aligned by the stable laminar gas flow.

On the basis of the aforementioned analysis, it is found that R_e could be decreased while R_i increased by decreasing the gas flux ϕ or increasing tube diameter d (in essence, the velocity v is depressed), which will be beneficial for ultralong SWNTs' growth due to a larger buoyancy and a stable gas flow. The larger the R_i, the greater the impact on the stability of the gas flow because it will cause a strong gas convection between different temperature locations. It is clear that the two functions are contradictory for growing well-aligned ultralong SWNTs. It means that we have to optimize the growth condition to obtain a suitable buoyancy that can lift the catalysts or grown SWNTs up into the laminar flow without introducing a strong effect on its stability. Therefore, it is critical to choose a suitable gas velocity (which means an appropriate R_i and R_e) for the growth of well aligned ultralong SWNTs.

B. Effects of the Quartz Tube Diameter d and Gas Flux ϕ on the Growth of Well-Aligned Ultralong SWNTs. To validate the analysis mentioned above, the quartz tube diameter d and gas flux ϕ were chosen as varied parameters for growing ultralong SWNTs. Figure 2 shows the SEM images of SWNTs grown in the quartz tube with $d = 12$ mm at different gas flux. Figure 2a shows an SEM image of SWNTs grown at the following condition: $FeCl_3$ as a catalyst precursor and a 40 sccm CH_4 and 80 sccm H_2 feed gas flow. In this situation, no ultralong SWNTs came out from the catalyst, whereas only thin SWNTs film appeared in the catalyst region. Even though Cu, which has been reported to have a higher SWNT growth activity than Fe does,[33] is applied as catalyst, still no ultralong SWNTs were observed (Figure 2b). Figure 2c,d shows SEM images of SWNTs grown at a 5 sccm CH_4 and 10 sccm H_2 feedstock using $FeCl_3$ and $CuCl_2$ as catalysts, respectively. Only short SWNTs of about 10 μm protruded from the catalyst region, and no orientated ultralong SWNTs were found. Further increasing or decreasing the gas flow does not show any improvement. The typical Raman spectrum in Figure 2e confirmed that the as-grown carbon nanotubes were SWNTs[34] and the D-band did not exist, which illustrated that the SWNTs were impurity-free and were provided with a perfect structure. The diameter distribution of about 40 SWNTs was measured by AFM and is shown in Figure 2f, which shows that the SWNTs' diameters are in the range of 1.2−2.2 nm.

Normally, the dynamic viscosity μ is 8.96×10^{-6} N·S/m^2 for hydrogen and 1.34×10^{-5} N·S/m^2 for methane at room temperature (298 K). According to the power law[30,31] in fluid mechanics, $\mu/\mu_0 = (T/T_0)^n$, where n is the power-law exponent and μ_0 is the dynamic viscosity at temperature T_0. Usually, n is 0.68 for hydrogen and 0.87 for methane; we can deduce μ for methane and hydrogen at the growth temperature of $T = 1243$ K. The calculated gas mixture density ρ is 0.0654 kg/m^{-3}, and the dynamic viscosity of gas mixtures μ_m is 4.5×10^{-5} N·S/m^2 at 1243 K.[35] Using eq 3, when the gas flux is 40 sccm CH_4 and 80 sccm H_2 in a 12 mm diameter quartz tube, R_e is 0.31, which is far smaller than 2000, but ultralong SWNTs are not obtained. When the gas flux is decreased to 5 sccm CH_4 and 10 sccm H_2, R_e is decreased to 0.039, but the R_i is 64 times larger than that of a 40 sccm CH_4 and 80 sccm H_2 gas flux, supposing that the gas density difference $\Delta\rho$ is the same as in the same vertical distance h. In this situation, although ultralong SWNTs cannot be grown, some short gas flow-directed SWNTs have come out from the catalyst and are stuck onto the substrate due to a large binding effect. We believe that, in a 12 mm diameter quartz tube, the buoyancy is not large enough to lift up the SWNTs because of a small temperature gradient between T_1 and T_2; thus, most carbon nanotubes attached onto the substrate surface and finally stopped growing. Apparently, the van der Waals interaction between the substrate and SWNTs is the primary reason to attach the SWNTs on the substrate and block the growth of gas flow-directed ultralong SWNTs.[32] To get rid of the binding effect of the substrate, we have changed the catalyst to regulate the reciprocal effect operated by the substrate, but still no ultralong SWNTs were obtained. Therefore, other factors besides the van der Waals effect must be taken into consideration for hampering the SWNTs' growth, to which we attributed the small buoyancy incapable of sustaining SWNTs in the gas flow.

Figure 3a shows an SEM image of SWNTs grown at 5 sccm CH_4 and 10 sccm H_2, applying $FeCl_3$ solution as a catalyst precursor in a 14 mm diameter quartz tube. We can observe that SWNTs of about 300 μm came out of the catalysts and short SWNTs curved and flourished in the catalyst region, which indicates that buoyancy begins to take effect when the quartz tube diameter is increased to 14 mm. Compared with experimental results in a 12 mm quartz tube, the R_i in a 14 mm quartz tube is greater when the gas flux is kept the same (supposing other parameters are not changed); namely, the buoyancy in this system is large enough to lift up the SWNTs or the catalysts. By increasing the gas flow to 8 sccm CH_4 and 16 sccm H_2, we can observe that much longer SWNTs (about 500 μm) came out of the catalysts than resulted with the smaller gas flux (shown in Figure 3b). It is probable that the carbon feedstock is not enough to grow longer SWNTs for the experiment with a lower CH_4 flow.

The interaction between catalyst and substrate plays an important role in the ultralong SWNTs' growth. Weaker interaction is favored for the growth of ultralong SWNTs because it is easier for the catalysts to float up higher above the substrate and move downstream along the gas flow. Much more SWNTs came out from catalysts possessing a weaker interaction against the substrate, such as Cu and Mn.[36,37] As shown in Figure 3c, longer SWNTs came out from catalysts and SWNTs agglomerated like wool, which indicates a weaker interaction between Mn and the silicon substrate compared with the situation of Fe catalysts.

Experiments were also carried out in 18, 22, and 37 mm diameter quartz tubes using the same ultralow gas flow as shown in Figure 2. Paying attention to the SEM results (Figure 4a,b), we saw that about millimeters ultralong and parallel SWNT arrays have been synthesized, demonstrating that the buoyancy was strong enough to sustain the long SWNTs in the laminar gas flow. When the diameter of the quartz tube is increased to 37 mm, only disordered ultralong SWNTs appear (shown in Figure 4c) compared with Figure 4a,b. In a 37 mm diameter quartz tube, the buoyancy is large enough to lift up the SWNTs; however, the orientation by the gas flow is damaged or destroyed. Supposing that the gas flow ϕ and the gas density difference $\Delta\rho$ in the same vertical distance h is the same for different diameter quartz tubes, the R_i ratio is about 90 between experiments carried out in a 37 mm diameter quartz tube and in a 12 mm diameter quartz tube, behaving in an ascending

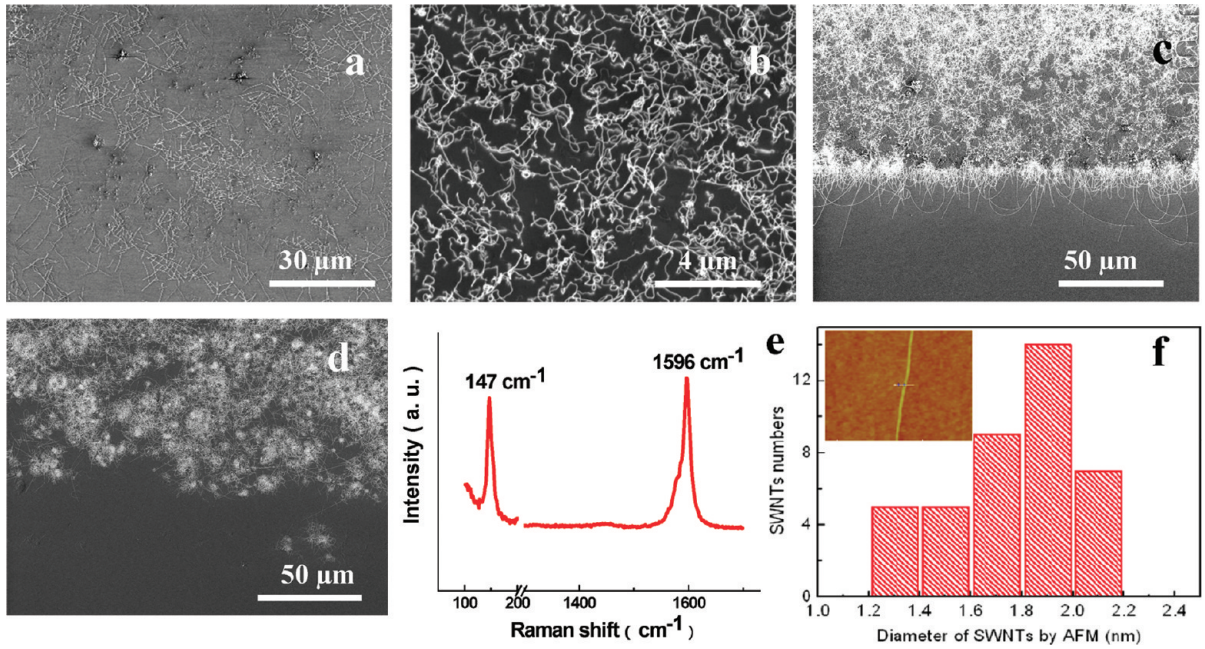

Figure 2. (a−d) Typical SEM images of SWNTs grown in a 12 mm inner diameter quartz tube. The growth conditions are (a) 0.01 M $FeCl_3$ catalyst, 40 sccm CH_4, and 80 sccm H_2; (b) 0.01 M $CuCl_2$ catalyst, 40 sccm CH_4, and 80 sccm H_2; (c) 0.01 M $FeCl_3$ catalyst, 5 sccm CH_4, and 10 sccm H_2; and (d) 0.01 M $CuCl_2$ catalyst, 5 sccm CH_4, and 10 sccm H_2. (e) Representative Raman spectrum of SWNTs on a SiO_2/Si substrate. Peaks at 147 and 1596 cm^{-1} are the RBM and G-band Raman shift of SWNTs. (f) Diameter distribution of SWNTs by AFM. The inset is a typical AFM image of an individual SWNT.

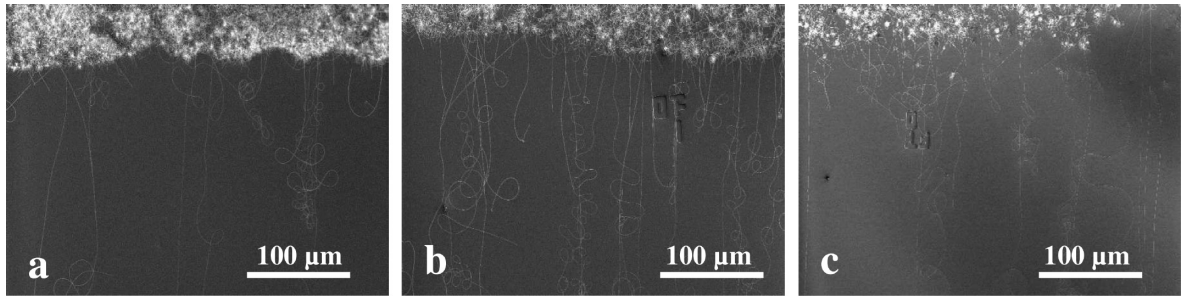

Figure 3. SEM images of SWNTs grown in a 14 mm diameter quartz tube. The growth conditions are (a) 0.01 M $FeCl_3$ catalyst, 5 sccm CH_4, and 10 sccm H_2; (b) 0.01 M $FeCl_3$ catalyst, 8 sccm CH_4, and 16 sccm H_2; and (c) 0.01 M $MnCl_2$ catalyst, 5 sccm CH_4, and 10 sccm H_2.

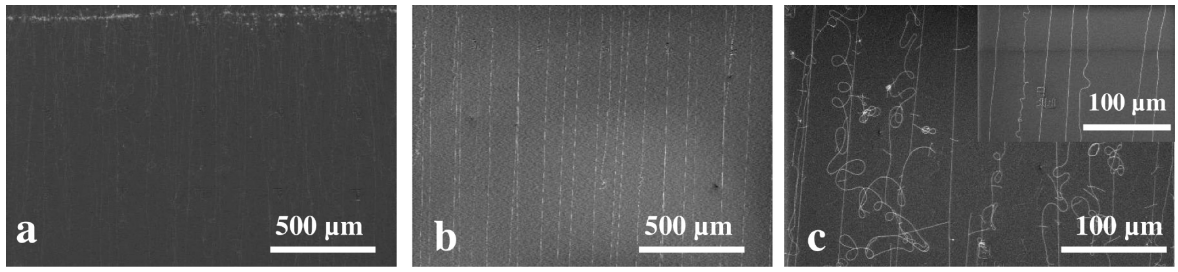

Figure 4. SEM images of ultralong SWNTs grown with 0.01 M $FeCl_3$ catalyst, 5 sccm CH_4, and 10 sccm H_2 in different tube diameters: (a) 18 mm tube, (b) 22 mm tube, and (c) 37 mm tube. Inset: SWNT SEM image with a tubule in a 37 mm tube.

trend when the diameter of the quartz tube increases. These results make it clear that a too large buoyancy is not preferred for growth of parallel ultralong SWNTs because it will affect the gas stability when gas convection takes place in the quartz tube, coherent with that we have analyzed through fluid mechanics.

As Philip et al[38] did, a small quartz tube (about 12 mm diameter) was put inside a larger diameter quartz tube to get better SWNT arrays on the substrate. Compared with Figure 2 in the same reaction condition, we got ultralong SWNT arrays (inset in Figure 4c), which illustrates a more stable gas flow and larger R_i in this tubule. In a tubule system, we presume that the gas velocity is uniform compared with the larger diameter outer tube and the R_i is the same as that without the inner quartz tube, but the R_e became smaller for the decreased quartz tube diameter. The above discussion validates that effect of buoyancy because the gas convection movement is reduced when a small diameter tube is introduced, and the growth

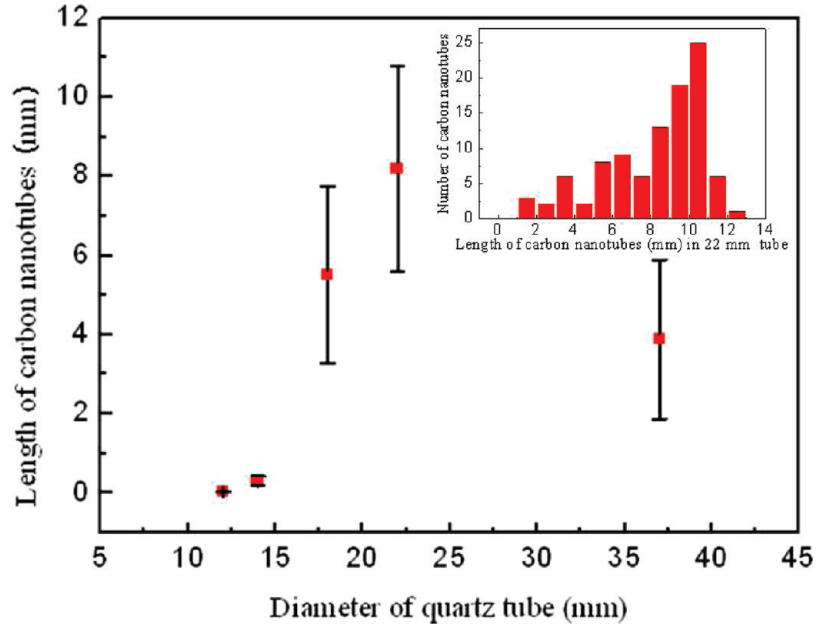

Figure 5. Average length of SWNTs grown in different inner diameter tubes with the same growth condition (the red square is the statistical average length of 100 random SWNTs for a specific sample, and the vertical line represents its standard deviation). The 22 mm diameter tube experiments got the best parallel and longest SWNT results. The inset shows the length distribution of 100 SWNTs in a 22 mm diameter quartz tube.

condition is greatly improved. In this situation, we can make use of the inner tube to get a more stable gas flow and better SWNT arrays. Under appropriate buoyancy, all SWNTs are well-aligned along the gas flow.

The experiments shown above can also be interpreted by boundary layer theory. For a larger diameter quartz tube with the same gas flux, the slower gas velocity will lead to a thicker boundary layer, resulting in a broader vertical range of temperature gradient where the buoyancy existed. That is why a larger buoyancy is attributed to a larger diameter quartz tube.

Figure 5 plots the average length of SWNTs against the inner diameter of quartz tubes at the same growth condition (0.01 M $FeCl_3$ catalyst, 5 sccm CH_4, and 10 sccm H_2) through experimental results. The inset in Figure 5 presents the length distribution of about 100 SWNTs grown in a 22 mm diameter quartz tube, displaying that half of the SWNTs reached 10 mm (due to substrate limitation, lengths exceeding 13 mm have not been counted). It showed that, in a 22 mm quartz tube, the longest SWNTs are obtained with a large standard deviation. Moreover, the 22 mm quartz tube brings the best SWNT alignment outcome among the five quartz tubes. The R_e and R_i ratio, compared with that of the 12 mm diameter quartz tube, clarified that the buoyancy is not so strong as to destroy the laminar gas flow, which means that the laminar gas flow condition and the buoyancy is optimal for the ultralong SWNTs growth among the experiments carried out in five different diameter quartz tubes.

In conclusion, we have systematically analyzed the effect of R_e and R_i on the growth of well-aligned ultralong SWNTs according to fluid dynamical properties of the CVD system and the SWNTs' floating growth model. By changing the quartz tube diameter and the gas flux for R_e and R_i variation, comparative CVD experimental results confirmed that a small R_e and a large R_i play an important role in growing well-aligned ultralong SWNTs. Our analysis indicated that an R_i-related buoyancy should be appropriate for the growth of ultralong SWNTs and the growth outcome can be controlled by tuning the gas flow velocity. We believe that this work will be a progress in the orientational growth of SWNTs on a substrate.

Acknowledgment. This work was supported by the NSFC (50972001, 20725307, and 50821061) and MOST (2006CB932701, 2006CB932403, and 2007CB936203). We thank B. Zhang, J. X. Hong, W. C. Tan, and X. C. Dai for their useful discussions.

References and Notes

(1) Baughman, R. H.; Zakhidov, A. A.; de Heer, W. A. *Science* **2002**, *297*, 787–792.
(2) Chen, Z. H.; Appenzeller, J.; Lin, Y. M.; Sippel-Oakley, J.; Rinzler, A. G.; Tang, J. Y.; Wind, S. J.; Solomon, P. M.; Avouris, P. *Science* **2006**, *311*, 1735.
(3) Tans, S. J.; Verschueren, A. R. M.; Dekker, C. *Nature* **1998**, *393*, 49–52.
(4) Collins, P. C.; Arnold, M. S.; Avouris, P. *Science* **2001**, *292*, 706–709.
(5) Bachtold, A.; Hadley, P.; Nakanishi, T.; Dekker, C. *Science* **2001**, *294*, 1317–1320.
(6) Rueckes, T.; Kim, K.; Joselevich, E.; Tseng, G. Y.; Cheung, C. L.; Lieber, C. M. *Science* **2000**, *289*, 94–97.
(7) Derycke, V.; Martel, R.; Appenzeller, J.; Avouris, P. *Nano Lett.* **2001**, *1*, 453–456.
(8) Ren, Z. F. *Nat. Nanotechnol.* **2007**, *2*, 17–18.
(9) Yao, Y. G.; Feng, C. Q.; Zhang, J.; Liu, Z. F. *Nano Lett.* **2009**, *9*, 1673–1677.
(10) Kang, S. J.; Kocabas, C.; Ozel, T.; Shim, M.; Pimparkar, N.; Alam, M. A.; Rotkin, S. V.; Rogers, J. A. *Nat. Nanotechnol.* **2007**, *2*, 230–236.
(11) Zhang, D. H.; Ryu, K.; Liu, X. L.; Polikarpov, E.; Ly, J.; Tompson, M. E.; Zhou, C. W. *Nano Lett.* **2006**, *6*, 1880–1886.
(12) Kocabas, C.; Shim, M.; Rogers, J. A. *J. Am. Chem. Soc.* **2006**, *128*, 4540–4541.
(13) Huang, L. M.; Jia, Z.; O'Brien, S. *J. Mater. Chem.* **2007**, *17*, 3863–3874.
(14) Ryu, K.; Badmaev, A.; Wang, C.; Lin, A.; Patil, N.; Gomez, L.; Kumar, A.; Mitra, S.; Wong, H. S. P.; Zhou, C. W. *Nano Lett.* **2009**, *9*, 189–197.
(15) Ding, L.; Yuan, D. N.; Liu, J. *J. Am. Chem. Soc.* **2008**, *130*, 5428–5429.
(16) Huang, S. M.; Woodson, M.; Smalley, R.; Liu, J. *Nano Lett.* **2004**, *4*, 1025–1028.

(17) Jiao, L. Y.; Fan, B.; Xian, X. J.; Wu, Z. Y.; Zhang, J.; Liu, Z. F. *J. Am. Chem. Soc.* **2008**, *130*, 12612–12613.

(18) Hur, S. H.; Park, O. O.; Rogers, J. A. *Appl. Phys. Lett.* **2005**, *86*, 243502–243504.

(19) Meitl, M. A.; Zhou, Y. X.; Gaur, A.; Jeon, S.; Usrey, M. L.; Strano, M. S.; Rogers, J. A. *Nano Lett.* **2004**, *4*, 1643–1647.

(20) Yao, Y. G.; Li, Q. W.; Zhang, J.; Liu, R.; Jiao, L. Y.; Zhu, Y. T.; Liu, Z. F. *Nat. Mater.* **2007**, *6*, 283–286.

(21) Chiu, P. W.; Kaempgen, M.; Roth, S. *Phys. Rev. Lett.* **2004**, *92*, 246802–246805.

(22) Wang, X. S.; Li, Q. Q.; Xie, J.; Jin, Z.; Wang, J. Y.; Li, Y.; Jiang, K. L.; Fan, S. S. *Nano Lett.* **2009**, *9*, 3137–3141.

(23) Yao, Y. G.; Dai, X. C.; Feng, C. Q.; ZHang, J.; Liang, X. L.; Ding, L.; Choi, W.; Choi, J. Y.; Kim, J. M.; Liu, Z. F. *Adv. Mater.* **2009**, *21*, 4158–4162.

(24) Zhang, B.; Hong, G.; Peng, B.; Zhang, J.; Choi, W.; Kim, J. M.; Choi, J. Y.; Liu, Z. *J. Phys. Chem. C* **2009**, *113*, 5341–5344.

(25) Yasuda, S.; Futaba, D. N.; Yamada, T.; Satou, J.; Shibuya, A.; Takai, H.; Arakawa, K.; Yumura, M.; Hata, K. *ACS Nano* **2009**, *3*, 4164–4170.

(26) Park, S.; Park, S.; So, H. M.; Jeon, E. K.; Park, D. W.; Kim, J. J.; S., K. B.; Kong, K. J.; Chang, H.; Lee, J. O. *Carbon* **2010**, *48*, 2218–2224.

(27) Huang, S. M.; Maynor, B.; Cai, X. Y.; Liu, J. *Adv. Mater.* **2003**, *15*, 1651–1655.

(28) Jin, Z.; Chu, H. B.; Wang, J. Y.; Hong, J. X.; Tan, W. C.; Li, Y. *Nano Lett.* **2007**, *7*, 2073–2079.

(29) Zheng, L. X.; O'Connell, M. J.; Doorn, S. K.; Liao, X. Z.; Zhao, Y. H.; Akhadov, E. A.; Hoffbauer, M. A.; Roop, B. J.; Jia, Q. X.; Dye, R. C.; Peterson, D. E.; Huang, S. M.; Liu, J.; Zhu, Y. T. *Nat. Mater.* **2004**, *3*, 673–676.

(30) Shaughhessy, E. J.; Katz, I. M.; Schaffer, J. P. *Introduction to Fluid Mechanics*; Oxford University Press: New York, 2005.

(31) Cebeci, T. *Convective Heat Transfer*, 2nd ed.; Horizons Publishing: Long Beach, CA, 2002.

(32) Hertel, T.; Walkup, R. E.; Avouris, P. *Phys. Rev. B* **1998**, *58*, 13870–13873.

(33) Zhou, W. W.; Han, Z. Y.; Wang, J. Y.; Zhang, Y.; Jin, Z.; Sun, X.; Zhang, Y. W.; Yan, C. H.; Li, Y. *Nano Lett.* **2006**, *6*, 2987–2990.

(34) Rao, A. M.; Richter, E.; Bandow, S.; Chase, B.; Eklund, P. C.; Williams, K. A.; Fang, S.; Subbaswamy, K. R.; Menon, M.; Thess, A.; Smalley, R. E.; Dresselhaus, G.; Dresselhaus, M. S. *Science* **1997**, *275*, 187–191.

(35) Wilke, C. R. *J. Chem. Phys.* **1950**, *18*, 517–519.

(36) Liu, B. L.; Ren, W. C.; Gao, L. B.; Li, S. S.; Liu, Q. F.; Jiang, C. B.; Cheng, H. M. *J. Phys. Chem. C* **2008**, *112*, 19231–19235.

(37) Yuan, D. N.; Ding, L.; Chu, H. B.; Feng, Y. Y.; McNicholas, T. P.; Liu, J. *Nano Lett.* **2008**, *8*, 2576–2579.

(38) Hong, B. H.; Lee, J. Y.; Beetz, T.; Zhu, Y. M.; Kim, P.; Kim, K. S. *J. Am. Chem. Soc.* **2005**, *127*, 15336–15337.

JP103731P